

Quantitative Identification of Mutant Alleles Derived from Lung Cancer in Plasma Cell-Free DNA via Anomaly Detection Using Deep Sequencing Data

Yoji Kukita¹, Junji Uchida², Shigeyuki Oba^{3,4}, Kazumi Nishino², Toru Kumagai², Kazuya Taniguchi¹, Takako Okuyama², Fumio Imamura², Kikuya Kato^{1*}

1 Research Institute, Osaka Medical Center for Cancer and Cardiovascular Diseases, Osaka, Osaka, Japan, **2** Department of Thoracic Oncology, Osaka Medical Center for Cancer and Cardiovascular Diseases, Osaka, Osaka, Japan, **3** Graduate School of Informatics, Kyoto University, Kyoto, Japan, **4** PRESTO, JST, Uji, Kyoto, Japan

Abstract

The detection of rare mutants using next generation sequencing has considerable potential for diagnostic applications. Detecting circulating tumor DNA is the foremost application of this approach. The major obstacle to its use is the high read error rate of next-generation sequencers. Rather than increasing the accuracy of final sequences, we detected rare mutations using a semiconductor sequencer and a set of anomaly detection criteria based on a statistical model of the read error rate at each error position. Statistical models were deduced from sequence data from normal samples. We detected epidermal growth factor receptor (*EGFR*) mutations in the plasma DNA of lung cancer patients. Single-pass deep sequencing (>100,000 reads) was able to detect one activating mutant allele in 10,000 normal alleles. We confirmed the method using 22 prospective and 155 retrospective samples, mostly consisting of DNA purified from plasma. A temporal analysis suggested potential applications for disease management and for therapeutic decision making to select epidermal growth factor receptor tyrosine kinase inhibitors (EGFR-TKI).

Citation: Kukita Y, Uchida J, Oba S, Nishino K, Kumagai T, et al. (2013) Quantitative Identification of Mutant Alleles Derived from Lung Cancer in Plasma Cell-Free DNA via Anomaly Detection Using Deep Sequencing Data. PLoS ONE 8(11): e81468. doi:10.1371/journal.pone.0081468

Editor: Raya Khanin, Memorial Sloan Kettering Cancer Center, United States of America

Received: March 16, 2013; **Accepted:** October 13, 2013; **Published:** November 21, 2013

Copyright: © 2013 Kukita et al. This is an open-access article distributed under the terms of the Creative Commons Attribution License, which permits unrestricted use, distribution, and reproduction in any medium, provided the original author and source are credited.

Funding: This work was supported by grants from Osaka Medical Center for Cancer and Cardiovascular Diseases. The funders had no role in study design, data collection and analysis, decision to publish, or preparation of the manuscript.

Competing interests: The authors have declared that no competing interests exist.

* E-mail: katou-ki@mc.pref.osaka.jp

Introduction

For some molecular targeted drugs against cancer, the examination of genomic changes in target genes has become a diagnostic routine and is indispensable for treatment decisions. For example, the strong effects of epidermal growth factor receptor tyrosine kinase inhibitors (EGFR-TKIs; i.e., gefitinib and erlotinib) on non-small-cell lung cancer (NSCLC) are correlated with activating somatic mutations in *EGFR* [1,2]. Patients who are administered these drugs are currently selected based on the presence of these activating mutations. The identification of the mutations is based on biopsy samples; the procedure is invasive and often difficult to perform. A non-invasive diagnostic procedure is desirable.

Cell-free DNA in the blood consists of DNA derived from cancer tissues and has been studied for non-invasive diagnostic procedures [3]. This DNA, termed circulating tumor DNA (ctDNA), is rare in blood, and its detection is a technical challenge. A number of methods have been examined, but

most of them have limitations in sensitivity and robustness. BEAMing (beads, emulsion, amplification and magnetics) [4] is most likely the most sensitive method. In BEAMing, PCR products amplified from a single molecule are fixed to a single magnetic bead using emulsion PCR. The mutation site is labeled with a fluorescent probe or primer extension, and the mutated allele is quantitatively detected by counting the fluorescently labeled beads. BEAMing successfully quantified *APC* and *KRAS* mutations in the ctDNA of colorectal cancer patients [5,6] and *EGFR* mutations in the ctDNA of lung cancer patients [7]. In spite of its high sensitivity and quantification ability, BEAMing has not gained in popularity because it is a laborious technology and requires oligonucleotides for each mutation position.

Because BEAMing and next-generation sequencers, i.e., massively parallel sequencers, use the same or a very similar template preparation technique, it is possible to apply next-generation sequencers for the same purpose. There have been several studies on the deep sequencing of cell-free DNA [8,9].

These studies suggested the possibility of the approach but lacked critical evaluation of the detection systems. In particular, they did not address the problem of multiple testing, which is inherent to diagnostic applications.

In this report, we established a method of detecting *EGFR* mutations in ctDNA in the peripheral blood of lung cancer patients using single-pass deep sequencing of amplified *EGFR* fragments. The recent development of a semiconductor sequencer (Ion Torrent PGM) [10] has addressed the shortcomings of other currently available sequencers (i.e., a long runtime for a single assay and high operating costs) and is applicable for diagnostic purposes. We applied anomaly detection [11,12] and determined a set of detection criteria based on a statistical model of the read error rate at each error position. The method quantitatively detected *EGFR* mutations in cell-free DNA at a level comparable to BEAMing, promising non-invasive diagnostics that complement biopsy.

Results

Principle of detection

Deep sequencing of a PCR-amplified fragment containing a mutation site can be conducted to detect and quantitate mutated alleles among the vast amounts of normal alleles derived from host tissues. The major problem associated with this approach is the frequency of errors introduced during sequencing and PCR amplification. The key issue here is the setting and accurate evaluation of detection limits. When the frequency of a base change at a target locus is higher than a predetermined read error rate (RER), we may judge the change to be due to the presence of a mutant sequence. That is, anomalies that fall significantly outside of the RER distribution are regarded as mutations. The RER is defined as the error rate calculated from final sequence data, including errors in both the sequencing and PCR steps. In anomaly detection [11,12], as in hypothesis testing, false positives are controlled based on a statistical model. In our case, the statistical model of the RER can be constructed from sequence data from the target regions of a sufficient number of normal individuals carrying no mutations.

If read errors occur under a probability distribution, the number of reads required to achieve a certain detection limit can be estimated. Figure 1a shows the relationship between the mutation detection limit, read depth, and RER at a significance level of $p=2 \times 10^{-5}$ for each individual detection without multiplicity correction, assuming that read errors occur following a Poisson distribution. The data illustrated in Figure 1a are supplied in Table S1. With an increasing read depth and decreasing RER, the detection limit decreases. In a previous study by our group [7], the detection limit for rare mutant alleles when using BEAMing [4] was 1 in 10,000 (0.01%). Because a plasma DNA assay sample contains approximately 5,000 molecules, this detection limit is reasonable. This goal can be achieved with 100,000 reads when the RER is below 0.01%.

Read error of the *EGFR* target region

For *EGFR*-TKI treatment, an activating *EGFR* mutation is indicative of treatment efficacy [1,2]. Patients to be

administered these drugs are currently selected based on the presence of these activating mutations. In addition to activating *EGFR* mutations, a resistant *EGFR* mutation known as T790M appears in approximately half of patients subjected to *EGFR*-TKI treatment [13,14]. Thus, three activating mutations, i.e., a deletion in *EGFR* exon 19 and L858R and L861Q in *EGFR* exon 21, as well as the T790M resistant mutation in *EGFR* exon 20 were selected as target loci.

We determined the RERs in a 169 base region around the target loci consisting by performing deep sequencing of DNA samples from normal individuals. We used an Ion Torrent PGM [10] sequencer for this work. Single-pass sequencing was performed, and the number of reads ranged from 44,400 to 373,000, averaging 162,000. We employed three types of DNA samples: 19 plasma DNA samples with amounts comparable to patients' samples, 16 leucocyte (white blood cell, WBC) DNA samples with amounts that were 10 or 50 times the size of a patient's sample, and 13 WBC DNA samples with amounts that were one-tenth the size of a patient's sample. We divided substitution errors into four patterns, corresponding to conversion to A, C, G, or T. Thus, there were 507 possible types of substitutions (169 base positions \times 3 patterns) in the target region. A substitution RER is graphically shown in Figure 1b, excluding the conversion from G to A at position 2,361 due to a frequent SNP. The substitution RERs are not uniform, nor are they independent from each other, and high RERs are associated with specific base positions. In addition, one substitution pattern is dominant at each base position. An insertion/deletion RER is graphically shown in Figure 1c. We did not distinguish between deletion and insertion errors, as insertions are often recognized as deletions and vice versa by the sequence alignment software. The insertion/deletion RER is generally higher than the substitution RER. A tendency similar to that of substitution is observed, in that high insertion/deletion RERs are associated with specific base positions. Figure 1d presents the distribution of the RERs. There were substantial differences between the substitution and insertion/deletion RERs. In 410 out of the possible 506 types of substitution (81.0%), the RER was lower than 0.01%. In contrast, out of the 169 types of insertions/deletion, the RER was lower than 0.01% in only 79 (46.7%). These results agreed with previously reported observations from the PGM platform [15]. The data illustrated in Figures 1b and 1c are supplied in Tables S2 and S3, respectively.

Due to high insertion/deletion read errors, we employed a specific method to detect the exon 19 deletion mutations. We prepared eight template exon 19 sequences with representative deletions and screened the deletion sequences by matching them with the template sequences. This method was quite effective for screening out read errors; no sequences with deletion read errors were found among the 48 samples tested.

Statistical models of read error rates and criteria for anomaly detection

We then examined statistical models of read error. In a Poisson distribution model, the average and variance of the number of incidences are expected to be the same and are

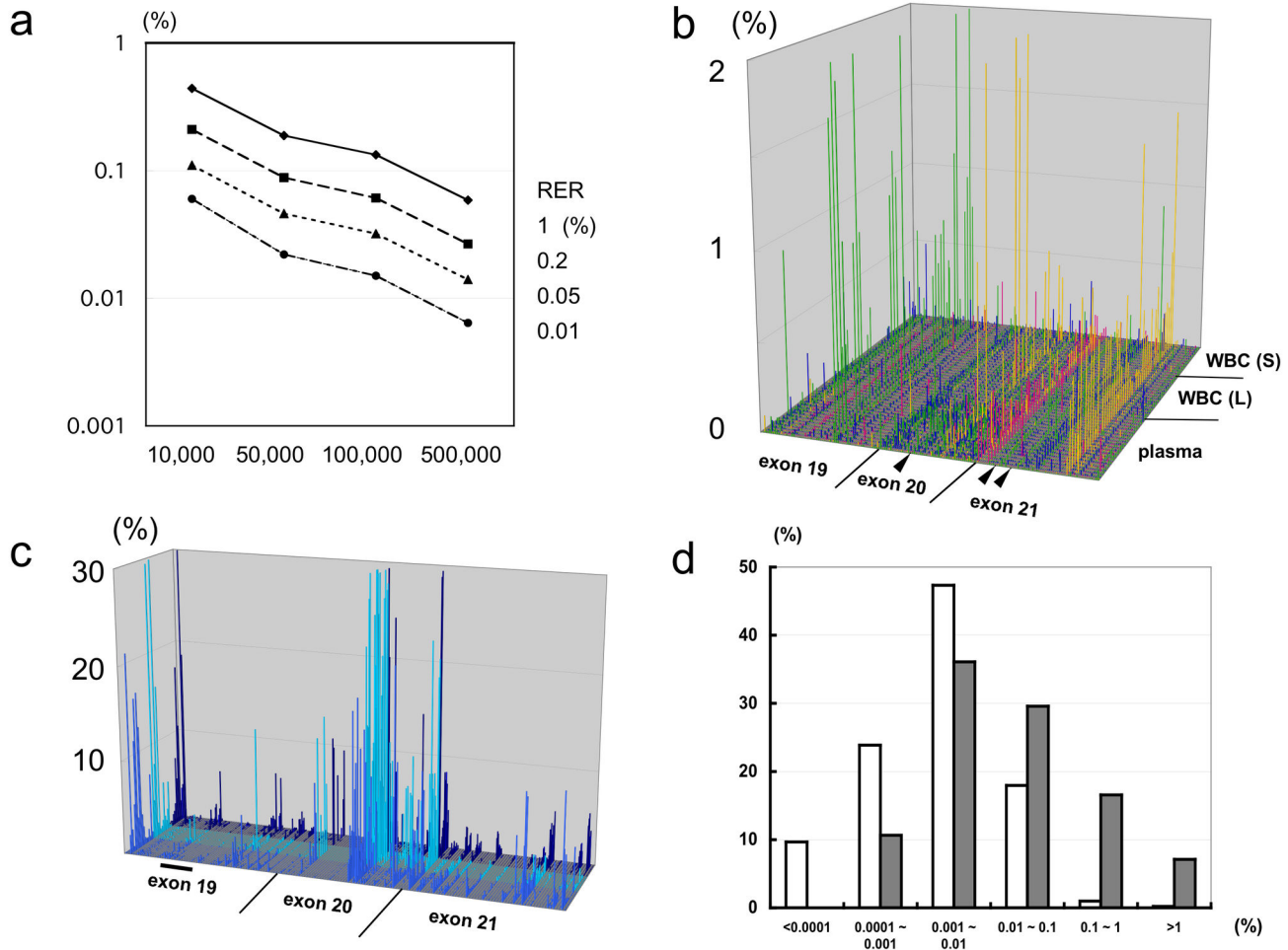


Figure 1. Read error of Ion Torrent PGM in the *EGFR* target region. a, Relationship between the read error rate, read depth, and detection limit for mutations when the significance level is $p=2 \times 10^{-5}$. Horizontal axis, read depth; vertical axis, detection limit (%). From top to bottom, each line indicates a read error rate (RER) of 1%, 0.2%, 0.05%, or 0.01%. b, Three-dimensional representation of substitution RER. x-axis, base positions of *EGFR* exons 19–21. From left to right, the arrowheads indicate the positions of T790M, L858R, and L861Q. y-axis, 48 DNA samples from normal individuals. From front to back, conversions to A (green), C (yellow), G (magenta), or T (blue) are aligned for each sample. z-axis, RER (%). c, Three-dimensional representation of the insertion/deletion error. x-axis, base positions of *EGFR* exons 19–21. The bar indicates the position of the exon 19 deletion. y-axis, 48 DNA samples from normal individuals. Blue, plasma DNA; light blue, WBC DNA (large amount); dark blue, WBC DNA (small amount). z-axis, RER (%). d, Distribution of the RER. White column, substitution error; gray column, insertion/deletion error. Horizontal axis, range of RER (%); vertical axis, incidence (%).

doi: 10.1371/journal.pone.0081468.g001

determined by the intensity parameter λ . Here, instead of using the RER, the read error incidence was presented as the incidence in 100,000 reads, and its average and variance at each base position were calculated. The relationships between the average and variance are shown in Figure 2a and Figure S1 in File S1 for the substitution and insertion/deletion read errors, respectively. In both cases, the variance becomes greater than the average in a considerable proportion of the cases. In these cases, application of the Poisson distribution would lead to increased numbers of false positives. This phenomenon, termed “overdispersion”, is common in biological

studies, and in such cases, a negative binomial distribution is applied [16]. Overdispersion is due to fluctuations of the intensity parameter, and it is rational to assume that the intensity parameter follows a gamma distribution. Under this scenario, the incidence number theoretically follows a negative binomial distribution. In Figure 2b, the increase in the threshold for substitution from a Poisson to a negative binomial distribution is plotted against the variance/average ratio of the read error for the substitution types whose variance/average ratio ranged from 1 to 2. When the ratio exceeded approximately 1.2-1.4, there were substantial increases in

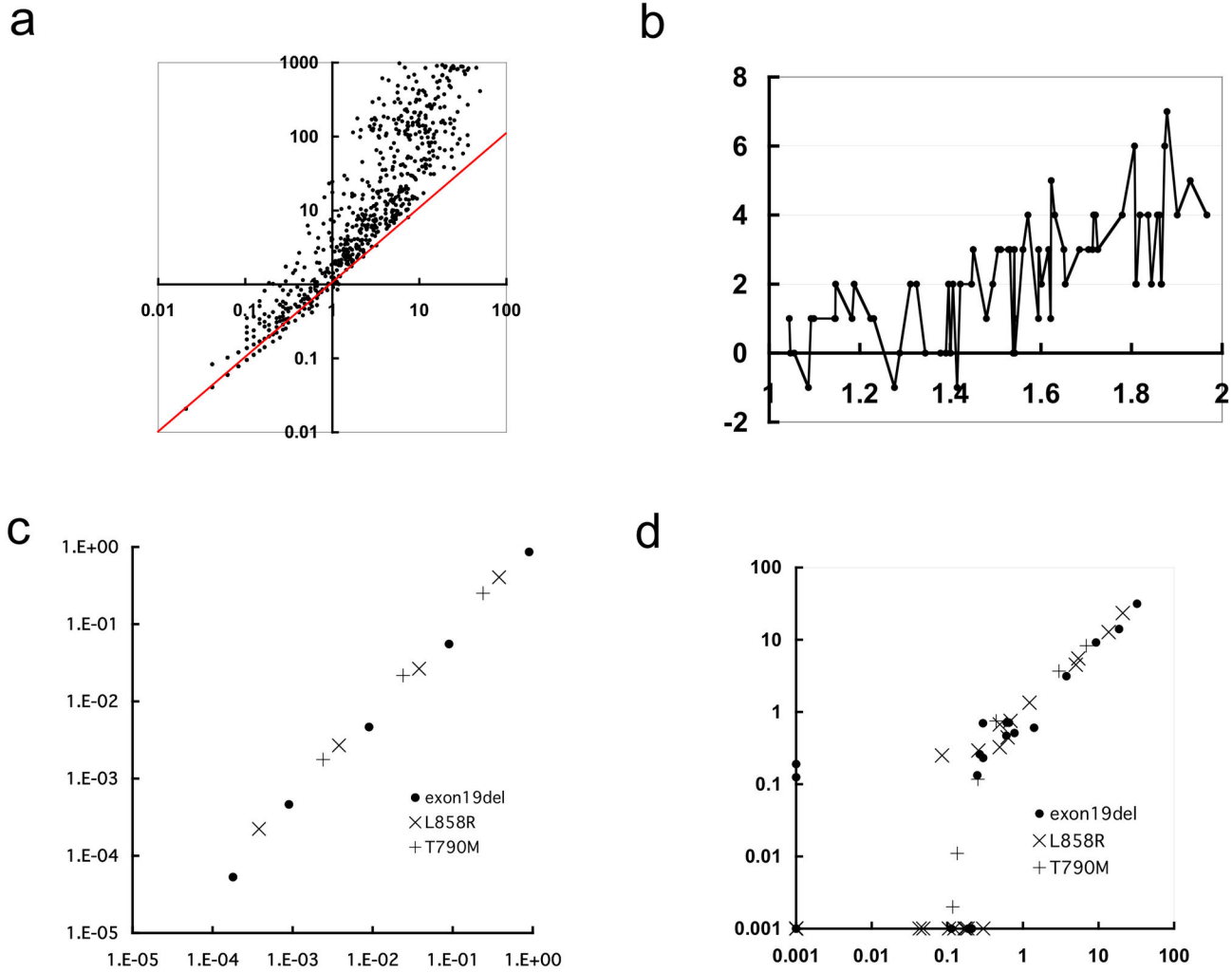


Figure 2. Characteristics of the mutation detection system. a, Relationship between the average and variance of the substitution error presented as the number per 100,000 reads. Horizontal axis, average; vertical axis, variance. The red line indicates where the average and variance are equal. b, Difference between thresholds calculated according to a negative binomial distribution and a Poisson distribution. The threshold is the minimum number of base changes in 100,000 reads meeting the level of statistical significance ($p=0.01$). Horizontal axis, variance/average ratio of the substitution read error; vertical axis, difference between thresholds. The types of substitutions whose variance/average ratio ranged from 1 to 2 are plotted. c, Accuracy of quantitation. Each data point represents the average of three assays. Horizontal axis, fraction of mutant alleles in artificial products; vertical axis, fraction of mutant alleles estimated from deep sequencing. d, Reproducibility of quantitation. Horizontal axis, base change rate in the first trial; vertical axis, base change rate in the second trial.

doi: 10.1371/journal.pone.0081468.g002

threshold. Thus, we constructed our statistical model of each substitution under the following criteria.

- 1 When the average read error in 100,000 reads was less than 1, a Poisson distribution with λ set to 1 was applied (169 types of substitutions).
- 2 When the average was greater than 1 and the variance/average ratio of the read error was less than 1.2, a Poisson distribution was applied (15 types of substitutions).
- 3 When the average was greater than 1 and the variance/average ratio of the read error was greater than 1.2, a negative binomial distribution was applied (323 types of substitutions).

The exon 19 deletion and L858R belonged to the first category, while the L861Q and T790M mutation sites belonged to the second and the third categories, respectively. The detection limits for the exon 19 deletion and the L858R, L861Q, and T790M substitution mutations at a significance level of $p=2 \times 10^{-5}$ were less than 0.01% and less than 0.01%, 0.01%, and 0.05%, respectively. In the following analysis, we used

$p=2 \times 10^{-5}$ as the significance threshold for each single detection, without considering a multiplicity correction, expecting one false positive in 50,000 samples.

The outline of the method is 1) amplification of *EGFR* fragments with exon-specific primers from plasma DNA; 2) deep sequencing of *EGFR* fragments with PGM (>100,000 reads / fragment), combining the PCR products; 3) matching the output sequences with *EGFR* template sequences; 4) detection of deletions and substitutions, and conversion of number of events into that in 100,000 reads; and 5) evaluation of the base changes with the anomaly detection criteria. In anomaly detection, the base changes are judged as mutations, when the number of events in 100,000 reads is equal to or exceeds the threshold value (exon 19 deletion, 7; L858R, 7; L861Q, 12; T790M, 60). A schematic representation is shown in Figure S2 in File S1.

Quantitativity and reproducibility

First, we examined the method's quantification ability. We prepared test samples including various fractions of PCR products of mutated *EGFR* fragments. There was a very good linearity ($r=0.998$) between the inoculated amounts of the PCR products and the observed mutant-to-normal allele ratios deduced from deep sequencing (Figure 2c). We then examined the reproducibility of the method using plasma samples from lung cancer patients whose primary lesions were confirmed to carry activating mutations. The fractions of the mutant alleles measured in two trials are plotted in Figure 2d. A high concordance ($r=0.989$) was observed, except in samples that contained small amounts of the mutant alleles, corresponding to an approximately 0.3% fraction of the alleles present or less. In these cases, the initial phase of PCR amplification was likely to be unsuccessful due to the low numbers of mutant templates, estimated at 15 copies or less. Thus, the limit of quantitation was approximately 0.3%.

Validation with samples from lung cancer patients

We further evaluated our method using lung cancer biopsy specimens, sampling plasma DNA and the primary lesion simultaneously as part of a prospective study. The results for the samples from 22 patients showed 86% concordance (95% confidence interval, 66 - 95), 78% (44 - 93) sensitivity, and 92% (66 - 98) specificity, setting the tissue biopsy as the standard. These results are promising with respect to the development of a diagnostic tool to complement lung cancer biopsy.

We then analyzed a total of 155 samples: 144 samples from plasma, eight from cerebrospinal fluid, and one each from urine, pleural effusion, and bronchial alveolar lavage. As for plasma samples, two or more samples were obtained from 32 patients at different time points of the disease courses. All of the obtained data are shown in Table S4. Clinical data of the patients including stage, histology, treatment, and status of resistance to EGFR-TKI are also listed in this Table. Among the 33 patients associated with a primary lesion containing the exon 19 deletion, this mutation was found in at least one of the plasma samples from 24 patients (72.7%). Of the 23 patients for which the primary lesions exhibited the L858R or L861Q substitutions, these mutations were found in at least one of the

plasma samples from 18 patients (78.2%). A double mutation (simultaneous detection of the exon 19 deletion and L858R) was observed in 12 plasma samples, although double mutations are not frequent in biopsy samples. Discrepancies between the activation mutation types identified in biopsy and plasma DNA samples were observed in five plasma samples. T790M was found in 13 out of 57 plasma samples (22.8%) from patients with EGFR-TKI resistance, and in 7 out of 87 plasma samples (8.0%) without EGFR-TKI resistance.

Temporal changes of *EGFR* mutation levels during the disease course

A considerable number of samples were collected from the same patient at different time points in the disease course. Temporal changes of *EGFR* mutation levels in plasma DNA from patients with three or more samples are schematically shown in Figure 3. Due to the relatively short sampling period, samples were obtained from only part of the disease course in most cases. We focused on two transitions: transition due to EGFR-TKI treatment initiation and that after acquiring EGFR-TKI resistance. Data before the treatment initiation was obtained in six cases. A significant decrease in the activation of mutation levels with the treatment was seen in all cases ($p=1.7 \times 10^{-4}$). Clearance of ctDNA by the treatment initiation is a general phenomenon.

Data were obtained both before and after acquiring EGFR-TKI resistance in seven cases. After acquiring resistance, the activation of mutation level was increased in five patients (218, 226, 259, 61, 66), decreased in one patient (44), and increased with delay in another patient (178). Increase of activation of mutations may correlate with disease progression. Despite the clear correlation between T790M and the EGFR-TKI-resistance status in the above validation study, dynamics of T790M during the disease course was not as clear as that of activation of mutations; T790M often appeared before acquiring resistance.

Three patients are described in more detail. Patient 226 was treated with gefitinib as first line chemotherapy. The gefitinib treatment was stopped several times due to adverse effects. A radiological response (partial response, PR) was observed from month 1 to month 9, and disease progression was observed in month 10. Prior to gefitinib treatment, the fraction of the mutant allele was very high (>50%), but after only one week of this treatment, the fraction of the mutant allele decreased to 0.3%, prior to any radiological changes (Figure S3a in File S1). T790M appeared at 10 months when disease progression began. Patient 243 also exhibited a skewed decrease in the mutant allele fraction at the initiation of gefitinib treatment (Figure S3b in File S1). This patient was treated with surgery and adjuvant chemotherapy (CDDP plus VNR) previously, and then subjected to gefitinib. Patient 41 presented with progression of neoplastic meningitis, and was subjected to combined erlotinib-pemetrexed therapy. Previous treatments were CDDP plus gemcitabine, gefitinib, and erlotinib. A minor radiological response was observed from months one to four, and disease progression occurred subsequently. There was a skewed decrease in the mutant allele fraction at the beginning of the therapy, and the increase upon disease progression was only slight (Figure S3c in File

Explore Litigation Insights

Docket Alarm provides insights to develop a more informed litigation strategy and the peace of mind of knowing you're on top of things.

Real-Time Litigation Alerts



Keep your litigation team up-to-date with **real-time alerts** and advanced team management tools built for the enterprise, all while greatly reducing PACER spend.

Our comprehensive service means we can handle Federal, State, and Administrative courts across the country.

Advanced Docket Research



With over 230 million records, Docket Alarm's cloud-native docket research platform finds what other services can't. Coverage includes Federal, State, plus PTAB, TTAB, ITC and NLRB decisions, all in one place.

Identify arguments that have been successful in the past with full text, pinpoint searching. Link to case law cited within any court document via Fastcase.

Analytics At Your Fingertips



Learn what happened the last time a particular judge, opposing counsel or company faced cases similar to yours.

Advanced out-of-the-box PTAB and TTAB analytics are always at your fingertips.

API

Docket Alarm offers a powerful API (application programming interface) to developers that want to integrate case filings into their apps.

LAW FIRMS

Build custom dashboards for your attorneys and clients with live data direct from the court.

Automate many repetitive legal tasks like conflict checks, document management, and marketing.

FINANCIAL INSTITUTIONS

Litigation and bankruptcy checks for companies and debtors.

E-DISCOVERY AND LEGAL VENDORS

Sync your system to PACER to automate legal marketing.